
Analysis and Simulation of Fuel Cell Powered Integrated Converter with Single Active Switch

*¹C. V. Vijay Kumar, ¹T. Sanjana, ¹B. Nagi Reddy

¹Department of EEE, Vignana Bharathi Institute of Technology, Hyderabad, India
*Email: cvvijay93@gmail.com

Abstract

Cascaded boost and Lou converters will serve as the foundation for this project's integrated converter, which will be driven by fuel cells and have a single active switch. The fact that the suggested converter is capable of delivering high levels of efficiency as well as voltage gains qualifies it for use in applications involving fuel cells. This converter offers a number of benefits, including a higher voltage gain ratio with no deployment of a transformer, improved efficiency, continued flow of input current, and the use of a single power switch. These benefits are derived from the fact that the converter only uses a single switch. The mode of continuous conduction is going to be investigated. Under steady-state conditions, the performance of the proposed DC-DC converter is analyzed and assessed. This performance is tested using the MATLAB to validate the proposed converter's capabilities in steady-state circumstances.

Keywords. DC-DC converter, fuel cell, high voltage gain, single switch integrated converter, continuous input current.

1. INTRODUCTION

The two basic categories of DC-DC topologies are isolated and non-isolated systems. Independent of the high value of the duty cycle, the turn ratio of the coils in the isolated topologies plays a crucial part in the rise in voltage gain. Sensitive loads are shielded from input source failures by the isolation that the high-frequency transformer's presence creates. The disadvantages of including a magnetic core include its increased bulk, weight, cost, and loss, notwithstanding the benefits described above. Additionally, the discontinuity in the input current and the presence of leaking inductors point to the need for snubber circuits, which raises the complexity and number of circuit components in the circuit. Therefore, when there is little justification for using an isolated circuit, it makes sense to use a non-isolated topology. The buck-boost and boost converters, which are among the classic non-isolated configurations and include buck-boost, buck, and boost converters, may step increase the input source's voltage level. The primary drawbacks of buck-boost converters include the discontinuous input and output currents and the output voltage's negative polarity. Because of this, the buck-boost converter experiences a pass-through rather than a step-up [1-3]. The input voltage gain can be increased by

using a typical boost converter. Theoretically, more orders of voltage gain can be attained by boosting the duty cycle and its proximity to unity. The conduction time of the diode approaches zero as the duty cycle gets closer to unity, which complicates the diode's reverse recovery time [4].

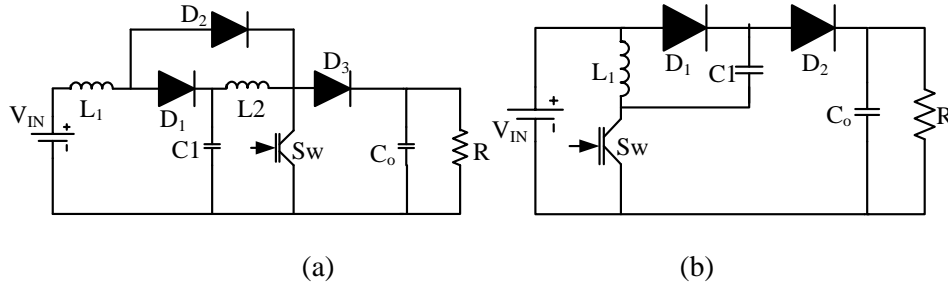


Figure 1. (a) Boosting topology, and (b) Luo circuit.

The aforementioned ideas provide the grounds for the birth of novel DC-DC converter topologies. The cascade of the boost converter is one of the provided structures and is shown in Figure 1a. Its topology, which was created by connecting two boost topologies, consisted of a switch and three diodes, as is clear [5]. When the duty-cycle gets closer to one in order to get more voltage gain, the number of parts can go up, which can have a big effect on efficiency. Figure 1b shows a Luo converter, which is another high step-up topology. The input current has a greater current ripple as compared to the boost topology, which raises the input DC-link capacitor's value. The diode is turned on because of the current created when the first capacitor and the source of power are connected in parallel. Additionally, a current ripple of this kind might shorten the capacitor's lifespan, which has an impact on the whole topology's longevity. Quadratic buck-boost topologies are introduced in [6]. The indicated converters of [6] had intermittent input currents; there were many inductors, and the voltage & current stress on the switching devices was substantial. The second sort of quadratic converter that has been recommended for fuel cell applications are the converters presented in [6]. A greater duty cycle value is necessary to obtain a significant voltage gain.

In this study, a cascaded boost and a Luo converter-based architecture are given. In contrast to the recommended converters [6], the developed converter's boost topology implementation in the first stage. Additionally, the suggested converters, and Luo converters are successful in solving the excessive current ripple of the input current. In the recommended topologies of [4-6], different amounts of inductor current travel through the input source. The voltage and current stresses on semiconductor components in the converter have decreased to a low, reachable value that is lower than unity [7-9]. As a result, the operating point has increased by more than 90%, and the planned topology's efficiency has reached high values.

2. PROPOSED INTEGRATED TOPOLOGY

Figure 2 illustrates the suggested topology's circuit diagram. The circuit first half employs the boost topology, results in a constant input current, which is the primary factor contributing to the developed converter's viability for usage in renewable energy applications. In the continuous conduction mode, the given architecture provides two operation modes (CCM). For analyzing, it is assumed that the converter is in steady-state. The first and third diodes are triggered in the first operating mode as a result the switch begins to conduct. The inductors are magnetised and have positive voltages at this time. Due to their respective negative currents, the converter's first and output capacitors have been discharged, while its second capacitor has been charged as a result of its positive current.

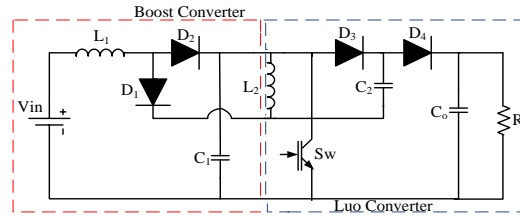


Figure 2. The proposed configuration.

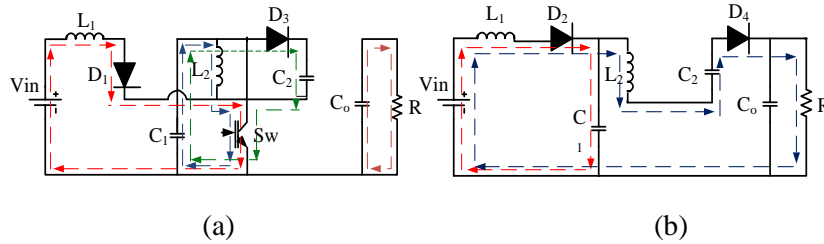


Figure 3. (a) Equivalent circuit of ON mode; (b) Equivalent circuit of OFF mode.

The 2nd and 4th diodes, however, begin to pass the current. In this mode, a negative voltage is given to the inductors. The inductors have therefore become demagnetized. The first and output capacitor currents have turned positive and are now beginning to charge. The equations at the inductors and capacitors are:

$$L_1 \frac{di_{L1}}{dt} = v_{in}D + (v_{in} - v_{c1})(1 - D) \quad (1)$$

$$L_2 \frac{di_{L2}}{dt} = v_{c1}D + (2v_{c1} - v_0)(1 - D) \quad (2)$$

$$C_1 \frac{dv_{C1}}{dt} = -(i_{L1} + i_{c2})D + (i_{L1} - i_{L2})(1 - D) \quad (3)$$

$$C_2 \frac{dv_{C2}}{dt} = i_{c2}D - i_{L2}(1 - D) \quad (4)$$

3. DEVICE STRESSES

The voltage second balance is used to compute the inductor voltage and the current second balance is used to calculate the capacitor current. They can be given as:

$$V_{c1} = \frac{V_{in}}{1 - D} \quad (5)$$

$$V_{c2} = \frac{V_{in}}{1 - D} \quad (6)$$

$$V_{c0} = \frac{(2 - D)V_{in}}{(1 - D)^2} \quad (7)$$

$$I_{L1} = \frac{(2 - D)}{(1 - D)} I_o \quad (8)$$

$$I_{L2} = \frac{1}{1 - D} I_o \quad (9)$$

Voltage/current stress on semiconductors is expressed using relationships such as duty cycle, input voltage, and output current. The difference between the highest and minimum inductor currents may be used to calculate the ripple inductor current. The difference between the highest and minimum capacitor voltages may also be used to compute the ripple in the capacitor voltage.

$$I_{D2} = \frac{(2 - D)I_o}{1 - D} \quad (10)$$

$$I_{D3} = I_{D4} = I_o \quad (11)$$

$$V_{S1} = V_{D3} = V_{D4} = \frac{V_{in}}{(1 - D)^2} \quad (12)$$

$$V_{D2} = \frac{V_{in}}{1 - D} \quad (13)$$

4. RESULTS & DISCUSSION

The projected converter is designed for an output power of 500W, with an output voltage of 200V. With the input voltage of 20V, the required output voltage with a gain of 10, can be produced at a duty ratio of 63%. To reduce the converter size, it is advisable to take higher switching frequencies (fs), however for the proposed simulation and design 50 kHz frequency is considered. With the considerable current and voltage ripples on the inductors and capacitors respectively, the energy component values are calculated and are observed in table 1. Figure 4 represents the input DC voltage waveform plotted using MATLAB simulation. A 20V DC input voltage is considered as the output of fuel cell to design the proposed converter.

Table 1 Simulation component values

S. No	Components	Step up mode
01)	Input Voltage (V_{in})	20 V
02)	Output Voltage (V_o)	200 V
03)	Output Power (P_o)	500 W
04)	Switching Frequency (F_s)	50 KHz
05)	Output Load R	80 ohms
06)	$M(D)=V_o/V_{in}$	10
07)	Duty cycle D	0.63
08)	$L_1(\Delta=1A)$	63 μH
09)	$L_2(\Delta=2A)$	340.54 μH
10)	$C_1(\Delta=2V)$	42.57 μF
11)	$C_2(\Delta=2V)$	25 μF
12)	$C_3(\Delta=5V)$	504 μF

The simulated voltage waveform of capacitor 1 (C_1) is shown in fig. 5. From the previous discussion, the capacitor (C_1) discharges the energy when the active switches are turned on, and charges when the switch is turned off. This phenomenon can be observed in the fig. 5, with a considerable peak ripple of 2V. Similarly, the simulated voltage waveform of capacitor 2 (C_2) is shown in fig. 6.

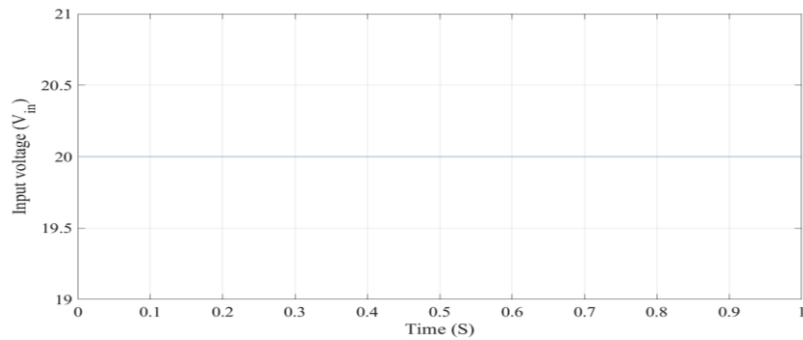


Figure 4. Simulated waveform of the input DC voltage

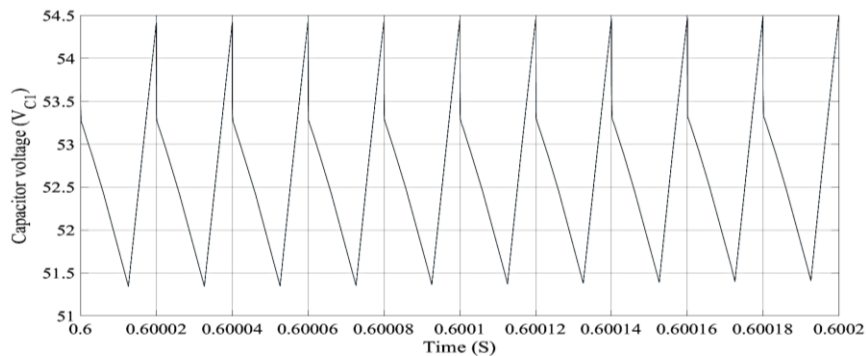


Figure 5. Simulated waveform of the capacitor 1 voltage with a peak ripple of 2V

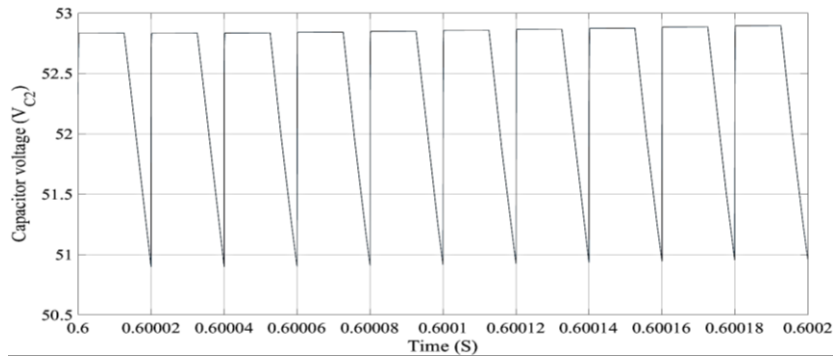


Figure 6. Simulated waveform of the capacitor 2 voltage with a peak ripple of 2V

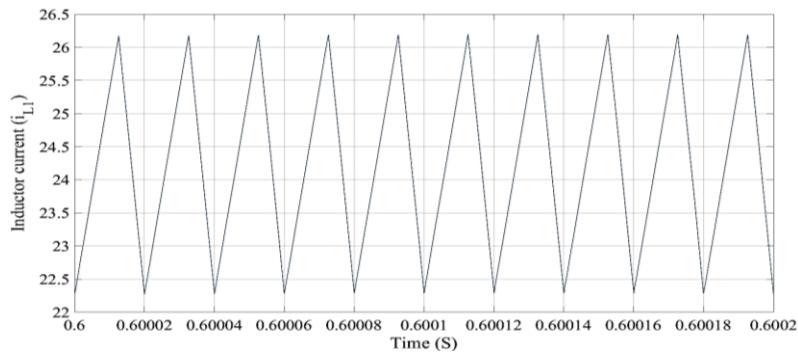


Figure 7. Inductor 1 (L_1) current waveform with a peak-to-peak ripple of 4 A

From the operation of the converter, the capacitor 2 (C_2) charges its energy when the active switches are turned on, and discharges when the switch is turned off. This phenomenon can be observed in the fig. 6, with a considerable peak ripple of 2V. Figures 7&8 shows the simulated inductor current waveforms i_{L1} & i_{L2} respectively under steady state operation (for 10 cycles). From fig. 7 it can be noted that the inductor L_1 peak to peak ripple is approximately 4A. This value is exactly matches to the theoretical consideration of inductor L_1 design.

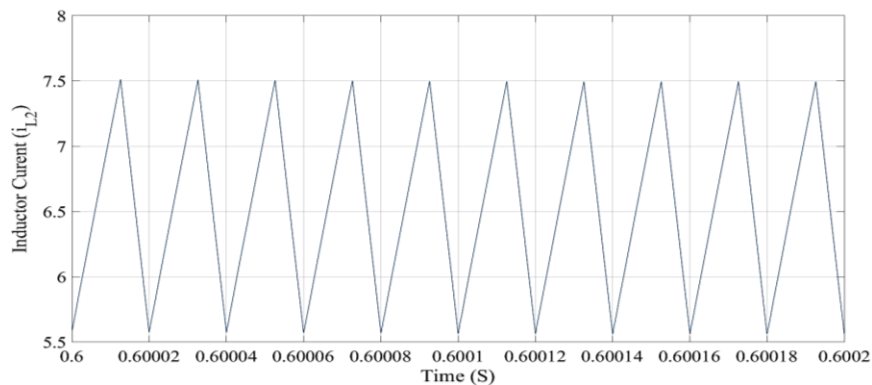


Figure 8. Inductor 2 (L_2) current waveform with a peak-to-peak ripple of 2 A

From fig. 8 it can be noted that the inductor L_2 peak to peak ripple is approximately 2A which exactly matches to the theoretical consideration of inductor L_2 . Figure 9 shows the simulated output current waveform with negligible ripple. The simulated value is approximately 2.42A and is much closed to the computed theoretical value. Figure 10 represents the simulated DC output voltage waveform with very low ripple (<0.5% approximately). The simulated value is approximately 194V and is much closed to the computed theoretical value.

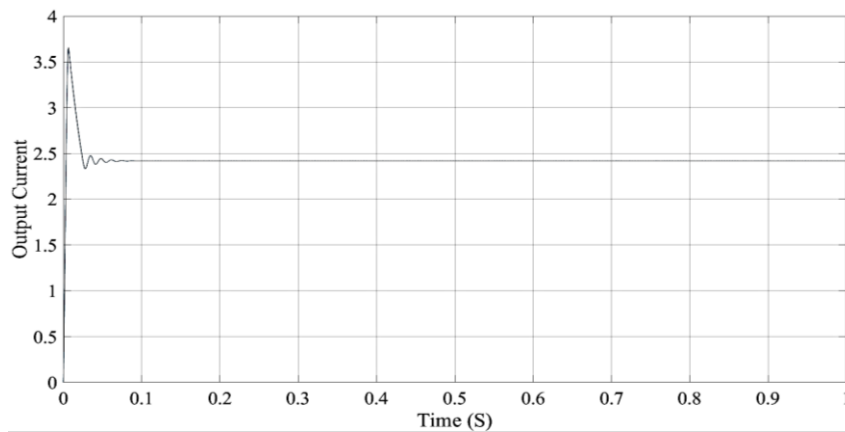


Figure 9. DC output current waveform of proposed topology

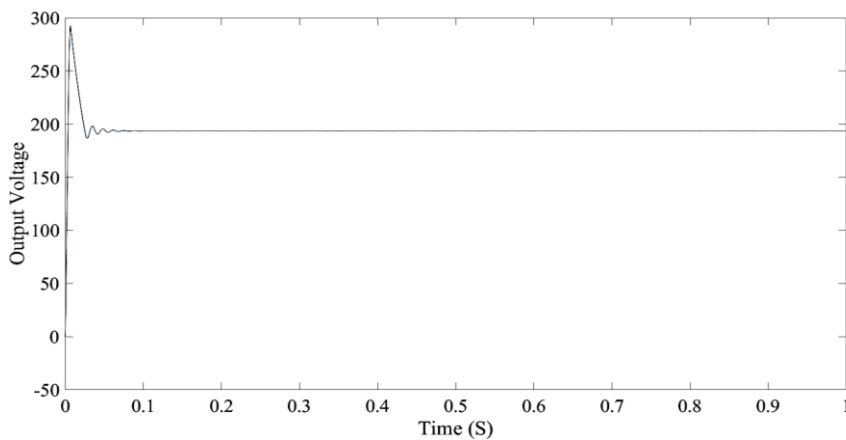


Figure 10. Output DC voltage waveform of proposed topology

5. CONCLUSION

In the paper, the formation of a step-up configuration was facilitated by the cascading of boost and Luo converters. It owns a variety of advantageous qualities, such as a high voltage conversion ratio without the requirement for transformers, high efficiency, stability in the input current, and the utilization of just one power switch. The configurations of the circuits, their operating principles, and how they

function in the mode of continuous conduction have been given. Simulation and analysis of performance are carried out by making use of theoretical values.

REFERENCES

- [1] Miao. S, Wang. F, Ma, X. “a new transformer less buck-boost converter with positive output voltage”, *IEEE Trans. Ind. Electron.*, 63, 2965–2975, 2016.
- [2] E. Salari, M. Banaei and A. Ajami, "Analysis of switched inductor three-level DC/DC converter", *Journal of Operation and Automation in Power Engineering*, vol. 6, no. 1, pp. 126-134, 2018.
- [3] Gopi, R.R, Sreejith. S, “Converter topologies in photovoltaic applications—A review”, *Renew. Sustain. Energy Rev*, 94, 1–14, 2018.
- [4] Nagi reddy. B, Sahithi Priya. Kosika, Manish patel. Gadam, jagadhishwar. Banoth, Ashok. Banoth, Srikanth goud. B, “Analysis of positive output buck-boost topology with extended conversion ratio”, *Journal of Energy Systems*, 6(1), pp. 62–83, 2022.
- [5] A. Tavassoli, B. Allahverdinejad, N. Rashidirad and M. Hamzeh, "Performance analysis of series SPOs in a droop-controlled DC microgrid", *2017 Smart Grid Conference (SGC)*, pp. 1-6, 2017.
- [6] Rosas-Caro. J.C, Valdez-Resendiz. J.E, Mayo-Maldonado. J.C, Alejo-Reyes. A, Valderrabano-Gonzalez. A, “Quadratic buck–boost converter with positive output voltage and minimum ripple point design”, *IET Power Electron.*, 11, 1306–1313, 2018.
- [7] V. Jagan, J. Kotturu and S. Das, "Enhanced-Boost Quasi-Z-Source Inverters with Two-Switched Impedance Networks," in *IEEE Transactions on Industrial Electronics*, vol. 64, no. 9, pp. 6885-6897, Sept. 2017, doi: 10.1109/TIE.2017.2688964.
- [8] A. Y. V. B. N. S. Naidu, S. Srinivas, V. Jagan and V. Sharma C., "Modified High Boost Quasi Z-Source Inverter with an Active Switched Network," *2020 IEEE Students Conference on Engineering & Systems (SCES)*, 2020, pp. 1-6, doi: 10.1109/SCES50439.2020.9236732.
- [9] Nagi Reddy, B., Chandra Sekhar, O., Ramamoorthy, M. “Analysis and implementation of single-stage buck-boost-buck converter for battery charging applications *Journal of Advanced Research in Dynamical and Control Systems*, 2018, 10(4), pp. 446–457.